SEUSS and *SEUSS-LIKE* Transcriptional Adaptors Regulate Floral and Embryonic Development in Arabidopsis[1][C][W][OA]

Fang Bao, Sridevi Azhakanandam, and Robert G. Franks*

Department of Genetics, North Carolina State University, Raleigh, North Carolina 27695

Multimeric protein complexes are required during development to regulate transcription and orchestrate cellular proliferation and differentiation. The Arabidopsis (*Arabidopsis thaliana*) *SEUSS* (*SEU*) gene encodes a transcriptional adaptor that shares sequence similarity with metazoan Lim domain-binding transcriptional adaptors. In Arabidopsis, *SEU* forms a physical complex with the LEUNIG transcriptional coregulator. This complex regulates a number of diverse developmental events, including proper specification of floral organ identity and number and the development of female reproductive tissues derived from the carpel margin meristem. In addition to *SEU*, there are three Arabidopsis *SEUSS-LIKE* (*SLK*) genes that encode putative transcriptional adaptors. To determine the functions of the *SLK* genes and to investigate the degree of functional redundancy between *SEU* and *SLK* genes, we characterized available *slk* mutant lines in Arabidopsis. Here, we show that mutations in any single *SLK* gene failed to condition an obvious morphological abnormality. However, by generating higher order mutant plants, we uncovered a degree of redundancy between the *SLK* genes and between *SLK* genes and *SEU*. We report a novel role for *SEU* and the *SLK* genes during embryonic development and show that the concomitant loss of both *SEU* and *SLK2* activities conditions severe embryonic and seedling defects characterized by a loss of the shoot apical meristem. Furthermore, we demonstrate that *SLK* gene function is required for proper development of vital female reproductive tissues derived from the carpel margin. We propose a model that posits that *SEU* and *SLK* genes support organ development from meristematic regions through two different pathways: one that facilitates auxin response and thus organ initiation and a second that sustains meristematic potential through the maintenance of *SHOOTMERISTEM-LESS* and *PHABULOSA* expression.

The control of transcriptional programs during development requires the action of multimeric protein complexes that interact with DNA regulatory regions and alter transcriptional efficiency. These complexes contain sequence-specific DNA-binding proteins that directly bind to the DNA as well as coregulatory proteins (coregulators or adaptors) that bridge interactions between the sequence-specific DNA-binding proteins and the general transcriptional machinery.

Lim domain-binding (Ldb) proteins are metazoan transcriptional adaptors required for a diversity of developmentally important events, including specification of chick neuronal identity and function of the amphibian Spemann organizer during dorsal/ventral polarity specification (Agulnick et al., 1996; Thaler et al., 2002; Matthews and Visvader, 2003). Ldb proteins have no known DNA-binding or enzymatic activities; rather, they function as adaptor proteins that provide protein interaction surfaces required for the assembly of multimeric regulatory complexes. Metazoan Ldb proteins contain a LIM-interaction domain (LID) required for interactions with LIM domain-containing proteins as well as a dimerization domain (DD) that supports the formation of higher order protein complexes (Fig. 1A; Agulnick et al., 1996; Jurata et al., 1996; Jurata and Gill, 1997). Ldb proteins also contain an Ldb1/Chip conserved domain (LCCD) that is contiguous with the dimerization domain. The LCCD was originally identified in the *Drosophila* Chip protein, a member of the Ldb adaptor family (van Meyel et al., 2003). The LCCD mediates the physical interaction of the Chip protein with another *Drosophila* transcriptional coregulator, Ssdp (for single-stranded DNA-binding protein).

The Arabidopsis (*Arabidopsis thaliana*) *SEUSS* (*SEU*) gene (AT1G43850) encodes a transcriptional adaptor that shares sequence similarity with the metazoan Ldb proteins throughout the DD and LCCD (Franks et al., 2002; Fig. 1A). However, SEU does not contain a recognizable LID, and there is no evidence of physical interactions between SEU and plant LIM domain-

[1] This work was supported by the National Science Foundation (grant nos. IOS 0416759 and IOS 0821896 to R.G.F.) and the U.S. Department of Agriculture Agricultural Research Service (grant no. NC06759).

* Corresponding author; e-mail rgfranks@ncsu.edu.

The author responsible for distribution of materials integral to the findings presented in this article in accordance with the policy described in the Instructions for Authors (www.plantphysiol.org) is: Robert G. Franks (rgfranks@ncsu.edu).

[C] Some figures in this article are displayed in color online but in black and white in the print edition.

[W] The online version of this article contains Web-only data.

[OA] Open Access articles can be viewed online without a subscription.

www.plantphysiol.org/cgi/doi/10.1104/pp.109.146183

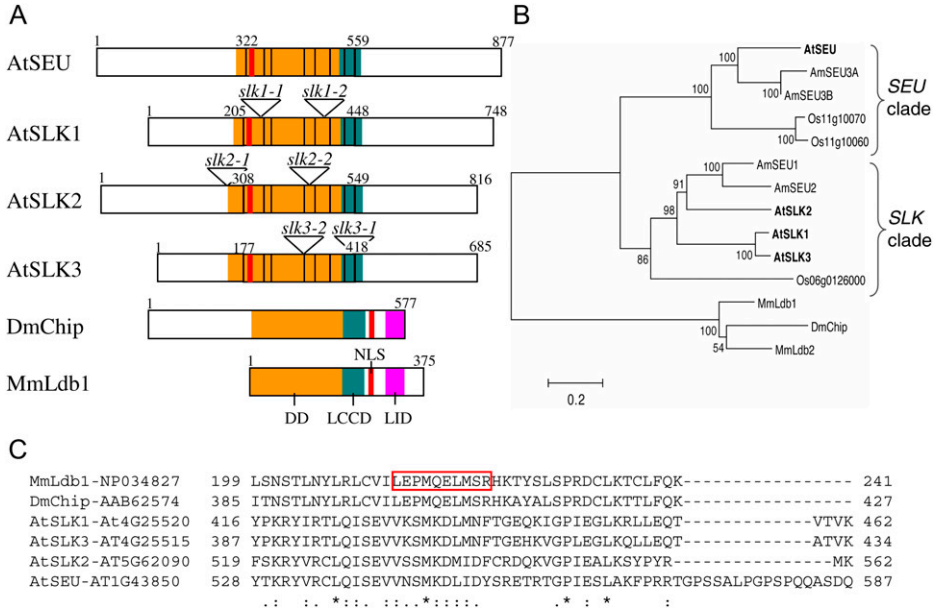

Figure 1. Structural and evolutionary relationships of SEU, SLK, and Ldb proteins. A, Conserved protein domains in AtSEU, AtSLK, and select metazoan Ldb proteins. The Arabidopsis proteins share sequence similarity to the DD of Ldb1 (orange) and the LCCD of Chip (teal). The LID domain in metazoan Ldb proteins (purple) does not appear to be conserved in the AtSEU and AtSLK proteins. Numbers indicate amino acid positions, and black dividing lines indicate the locations of exon/exon boundaries that are conserved in the Arabidopsis proteins. Mutant allele insertion sites are indicated for *SLK* genes. B, The evolutionary history of full-length *SLK* proteins inferred using the neighbor-joining method (Saitou and Nei, 1987). The optimal tree (shown) suggests that the AtSLK proteins fall into a clade that is distinct from that containing AtSEU. The percentages of bootstrap support are shown next to the branches (Felsenstein, 1985). Evolutionary distances are in units of number of amino acid substitutions per site. C, ClustalW2 analysis of the LCCD region of metazoan Ldb and Arabidopsis SLK proteins. LCCD spans amino acids 201 to 249 in MmLdb1 and 387 to 435 in DmChip; the red boxed area indicates 10 amino acids deleted from Ldb1 that specifically disrupt activity of LCCD (van Meyel et al., 2003). At, *Arabidopsis thaliana*; Am, *Antirrhinum majus*; Dm, *Drosophila melanogaster*; Mm, *Mus musculus*; NLS, nuclear localization signal; Os, *Oryza sativa*. Protein identifiers not listed above are as follows: MmLdb2, NP034828; Os06g0126000, NP_001056655; Os11g10060, ABA91996; Os11g10070, ABA91997; AmSEU1, AJ620907; AMSEU2, AJ620908; AmSEU3A, AJ620909; AmSEU3B, AJ620910.

containing proteins. In Arabidopsis, the SEU LCCD likely supports a physical interaction between SEU and two paralogous transcriptional coregulators: LEUNIG (LUG) and LEUNIG_HOMOLOGUE (LUH; Sridhar et al., 2004, 2006; Sitaraman et al., 2008). The Arabidopsis LUG and LUH proteins share a conserved domain with the metazoan Ssdp proteins, and this domain is required for physical interactions between LUG and SEU in Arabidopsis and Ssdp and Ldb1 in metazoans (Conner and Liu, 2000; van Meyel et al., 2003; Sridhar et al., 2004). Thus, the LCCD portion of the SEU protein likely mediates a set of protein-protein interactions that are functionally conserved across the plant and animal kingdoms (van Meyel et al., 2003).

The Arabidopsis *SEU* gene encodes a nucleus-localized protein that is expressed widely throughout many developmental stages and tissues (Franks et al., 2002; Azhakanandam et al., 2008). Functional analyses indicate that *SEU* plays multiple roles during Arabidopsis development. The most well characterized of these is a role for *SEU* in the repression of *AGAMOUS* (*AG*) during floral organ identity specification (Franks et al., 2002). Within the developing flower, the SEU/LUG protein complex physically interacts with pairs of MADS domain DNA-binding proteins (i.e. SEPALATA3, APETALA1, SHORT VEGETATIVE PHASE1, and AGAMOUS-LIKE24) that bind to *AG* regulatory sequences (Gregis et al., 2006; Sridhar et al., 2006). LUG then recruits HDA19, a class 1 histone deacetylase, as well as components of the Mediator complex to bring about repression of *AG* transcription in the perianth (nonreproductive) floral organs (Gonzalez et al., 2007).

SEU also functions during the development of the carpel margin meristem (CMM; Azhakanandam et al., 2008). The CMM (also termed the medial ridge of the gynoecium) is a vital meristematic structure that is located on the margins of the fused Arabidopsis carpels and gives rise to several critical female reproductive structures including the ovules, the septum, and the transmitting tract (Bowman et al., 1999). *SEU* functions in a partially redundant manner with a number of other transcriptional regulators, including *AINTEGUMENTA* (*ANT*), *FILAMENTOUS FLOWER*/

YABBY1 (*FIL/YAB1*), and *LUG*, during the development of the CMM (Liu et al., 2000; Nole-Wilson and Krizek, 2006; Azhakanandam et al., 2008). The analysis of *lug ant* and *seu ant* double mutant gynoecia indicates that the disruption of CMM development in these genotypes is not caused by ectopic *AG* expression (Liu et al., 2000; Azhakanandam et al., 2008). Rather, these experiments support a model in which *SEU*, *LUG*, and *ANT* maintain the expression of the adaxial fate determinant *PHABULOSA* (*PHB*) and thus reinforce polarity specification within the gynoecium. Thus, the SEU and LUG coregulators participate in a diversity of transcriptional events during varied developmental processes in a manner analogous to that of the Ldb and SSDP metazoan proteins (van Meyel et al., 2003).

SEU is also required for phenotypic and transcriptional responses to the auxin class of plant hormones (Pfluger and Zambryski, 2004). The *seu* mutant seedlings display a reduced sensitivity to applied auxin as well as a variety of auxin-resistant growth phenotypes. Furthermore, the expression of the auxin-sensitive DR5:GUS reporter (Ulmasov et al., 1997) was reduced in *seu* mutant roots relative to wild-type roots (Pfluger and Zambryski, 2004). SEU was shown to physically interact with ETTIN/AUXIN RESPONSE FACTOR3 (ETT/ARF3) in a yeast two-hybrid assay (Pfluger and Zambryski, 2004). ETT/ARF3 is a member of a family of transcription factors that bind to auxin response elements located in the regulatory regions of auxin-responsive genes (Sessions et al., 1997). Thus, the physical interaction between SEU and ETT suggests a potential direct role for *SEU* during auxin response.

In addition to *SEU*, there are three Arabidopsis *SEUSS-LIKE* (*SLK*) genes that encode putative transcriptional adaptors containing a Ldb-type DD followed by an LCCD: *SLK1* (AT4G25520), *SLK2* (AT5G62090), and *SLK3* (AT4G25515; Franks et al., 2002; Fig. 1A). The sequence similarity between *SEU* and the *SLK* genes suggests that they may share functional redundancy. Putative *Antirrhinum* orthologs of *SEU* and the *SLK* genes physically interact with *STYLOSA*, the *Antirrhinum LUG* ortholog; however, mutations in the *Antirrhinum SLK* genes and *SEU* have not been isolated (Navarro et al., 2004).

To determine the functions of the *SLK* genes and investigate the degree of functional redundancy between *SEU* and *SLK* genes, we characterized available *slk* mutant lines in Arabidopsis. Here, we show that mutations in any single *SLK* gene failed to condition an obvious morphological abnormality. However, by generating higher order mutant plants, we uncovered a degree of redundancy between the *SLK* genes and between *SLK* genes and *SEU*. Notably, the concomitant loss of both *SEU* and *SLK2* activities results in severe embryonic and seedling defects that are characterized by a loss of all structures derived from the shoot apical meristem (SAM). These observations suggest a previously unrecognized role for *SEU* and the *SLK* genes during embryonic development. We also demonstrate that *SLK* genes function in the development of the CMM in a manner that is similar to that of *SEU*. We propose a model that suggests that *SEU* and *SLK* genes support organ development from meristematic regions through two different pathways: one that facilitates auxin response and thus organ initiation and a second that sustains meristematic potential through the maintenance of *SHOOTMERISTEM-LESS* (*STM*) and *PHB* expression.

RESULTS

Structural and Phylogenetic Analyses of SEU, SLK, and Ldb Proteins

The three Arabidopsis *SLK* genes and *SEU* all encode putative transcriptional adaptors that share sequence similarity to the Ldb family of transcriptional regulators within the DD and LCCD (Franks et al., 2002; Fig. 1A). Outside of the DD and LCCD, the three *SLK* genes share significant sequence similarity with each other, but their sequences diverge from *SEU*. Thus, the three *SLK* genes are more similar to each other than they are to *SEU*. This became more apparent when we employed a neighbor-joining method to generate a phylogeny for this group of transcriptional regulators including members from other monocot and dicot species. This analysis supports the separation of the *SLK* genes into a phylogenetic clade (*SLK* clade) that is distinct from that of *SEU* (*SEU* clade; Fig. 1B). A protein sequence similarity/identity matrix also supports the differentiation of the *SEU* and *SLK* clades (Table I). The percentage identity between *AtSEU* and the putative rice (*Oryza sativa*) SEU ortholog Os11g10060 is higher than it is between *AtSEU* and the Arabidopsis *SLK* genes (Table I). The apparent sequence divergence in the N- and C-terminal portions suggests that these protein regions may support functional differences between the SEU and SLK clade members. The *SLK1* and *SLK3* genes appear to have arisen from a tandem duplication event on chromosome 4 and encode highly similar proteins (greater than 80% similarity). For this article, we use the term "*SLK* genes" to describe genes in the *SLK* clade (i.e. *SLK1*, *SLK2*, and *SLK3* in Arabidopsis) and the term "*SEUSS*-related genes" to describe the larger gene family that includes members of both clades. Interestingly, the rice and snapdragon (*Antirrhinum majus*) genomes encode at least two paralogs in the *SEU* clade, while *AtSEU* is the only paralog found in the *SEU* clade in Arabidopsis. We carried out ClustalW2 analysis to more closely examine the sequence similarity within the LCCD of SEU, the SLK proteins, and the metazoan Ldb proteins (Fig. 1C). Our analysis indicates that the LCCD sequence is conserved in SEU as well as in the three SLK proteins and suggests that the SLK proteins may physically interact with LUG as well as with the LUH protein, another Arabidopsis coregulator that is structurally related to LUG

Table I. *Amino acid similarity and identity (% similarity/% identity) across three conserved portions of selected SEU-related proteins*

Portion	SEU	SLK1	SLK2	SLK3	Os11g10060	Os06g0126000
N-terminal portion[a]						
SEU	XXX	39/27	45/25	35/25	58/41	36/24
SLK1	39/27	XXX	48/37	83/79	34/26	58/34
SLK2	45/25	48/37	XXX	44/33	41/26	47/34
SLK3	35/25	83/79	44/33	XXX	30/24	55/33
Os11g10060	58/41	34/26	41/26	30/24	XXX	36/21
Os06g0126000	36/24	58/34	47/34	55/33	36/21	XXX
Dimerization and LCCD portion[b]						
SEU	XXX	76/55	76/58	76/54	89/82	72/49
SLK1	76/55	XXX	86/72	99/97	73/55	75/54
SLK2	76/58	86/72	XXX	85/71	74/57	76/53
SLK3	76/54	99/97	85/71	XXX	74/55	76/54
Os11g10060	89/82	73/55	74/57	74/55	XXX	71/49
Os06g0126000	72/49	75/54	76/53	76/54	71/49	XXX
C-terminal portion[c]						
SEU	XXX	40/23	39/23	38/24	52/32	41/17
SLK1	40/23	XXX	48/32	80/75	36/21	42/26
SLK2	39/23	48/32	XXX	50/33	35/20	40/25
SLK3	38/24	80/75	50/33	XXX	35/21	42/27
Os11g10060	52/32	36/21	35/20	35/21	XXX	37/18
Os06g0126000	41/17	42/26	40/25	42/27	37/18	XXX

[a]Amino acids 1 to 322 in SEU. [b]Amino acids 323 to 570 in SEU. [c]Amino acids 571 to 877 in SEU.

(Sitaraman et al., 2008). Recently, Stahle et al. (2009) reported that SEU and the SLK proteins can interact with LUG and LUH in a yeast two-hybrid assay.

SLK1 Shares Redundant Functions with *SEU* during Flower and Gynoecium Development

To investigate the functions of the *SLK* genes in Arabidopsis, we characterized three independent mutant alleles of *SLK1* (*slk1-1*, *slk1-2*, and *slk1-3*) and two mutant alleles of *SLK2* (*slk2-1* and *slk2-2*) and *SLK3* (*slk3-1* and *slk3-2*; see "Materials and Methods"; Fig. 1; Supplemental Table S1; Alonso et al., 2003). Our analysis indicated that homozygous loss-of-function mutations in these alleles do not condition any obvious morphological abnormalities (Fig. 2; data not shown). The *slk1-1* allele is a strong loss-of-function allele that expresses *SLK1* mRNA at 30% of wild-type levels and is predicted to encode a truncated protein product containing 242 of 748 amino acids that would lack most of the DD and LCCD (Fig. 1; Supplemental Fig. S2). The *slk1-2* allele did not display reduced levels of mRNA but is predicted to truncate the protein at amino acid 387. Our quantitative real-time PCR (qRT-PCR) analysis indicated that the *slk2-1* allele was a near null mutant, expressing only 0.4% of the wild-type level of *SLK2* mRNA. The *slk2-2*, *slk3-1*, and *slk3-2* alleles are not RNA null alleles but are predicted to be hypomorphic alleles with insertions after amino acid 455 of *SLK2* and in intron 8 and intron 4 of *SLK3*, respectively. Except where otherwise noted, we used *slk1-1* and *slk2-1* alleles for phenotypic analysis. Our preliminary data suggest that the *slk3-1* mutant line contains a reciprocal chromosomal translocation that can be found in a subset of the T-DNA mutant lines (Curtis et al., 2009), complicating the construction of higher order mutants. We report data for only the *slk3-1* and *slk3-2* homozygous single mutants in this paper.

To investigate functional redundancy between *SEU* and members of the *SLK* gene family, we created a collection of higher order mutants. Like the *slk1*, *slk2*, and *slk3* single mutant plants, the *slk1 slk2* double mutants also did not display an observable morphological phenotype (Fig. 2, B and K). Interestingly, the *seu slk1* and *seu slk2* double mutants did display phenotypic enhancements (relative to the *seu* single mutant phenotype) in several aspects of plant development.

The *seu slk1* plants are shorter in stature than the *seu* and *slk1* single mutants and are sterile (Fig. 2G). The *seu slk1* double mutants also displayed enhanced disruptions of floral development. This was characterized by a reduction in organ numbers in whorls 2, 3, and 4 and weak homeotic organ identity transformations in 2% of whorl 1 organs (Table II). The majority (74%) of whorl 2 organs were filaments or filamentous petals (Fig. 2, D and F, arrowheads). Disruption of gynoecial morphology in the *seu slk1* double mutant was somewhat variable but was consistently more severe than in the *seu* and *slk1* single mutants, with a greater degree of splitting at the gynoecial apex. In 18% of the *seu slk1* flowers, the gynoecium was made up of a single carpel that was fused along its margins into a tube (Fig. 2E). Additionally, we observed a short-valve phenotype in 41% (n = 128) of the carpels in which the basal boundary of the valve was shifted toward the gynoe-

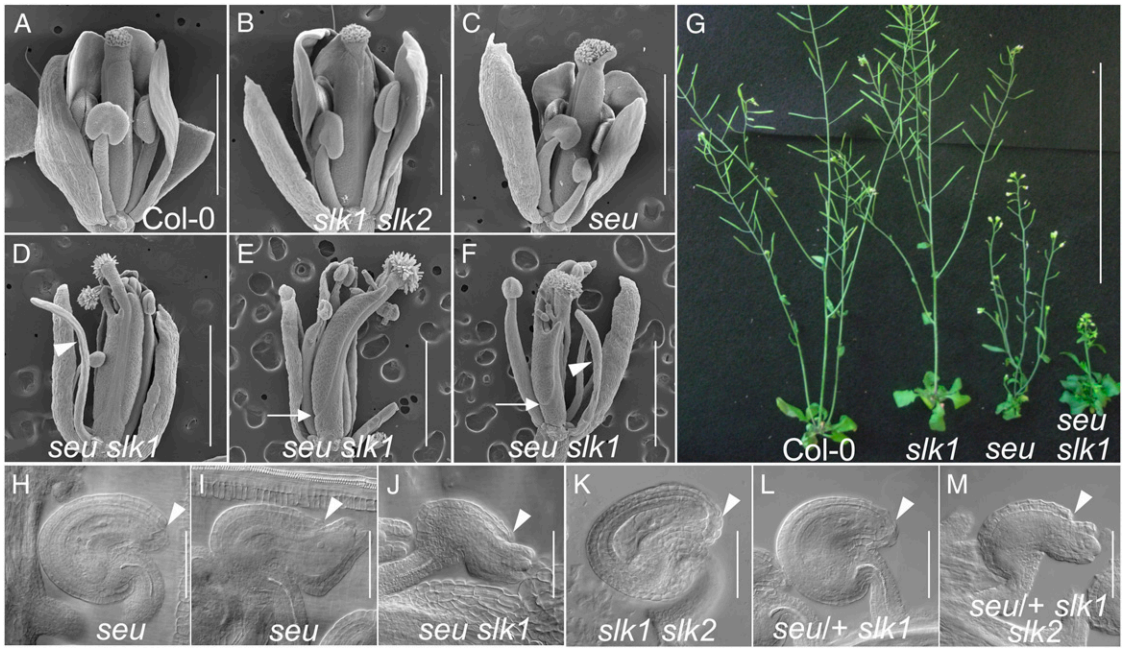

Figure 2. *SLK1* shares redundant function with *SEU* during gynoecium and ovule development. A to F, Scanning electron micrograph images of flowers of the indicated genotypes. Bars = 1 mm. Some organs from the front of the flower have been removed to image internal whorls. D to F show three *seu slk1* double mutant flowers that display enhanced splitting of the gynoecial apices and narrow or filamentous petals (arrowheads). Arrows indicate the basal extent of the carpel valves that is shifted toward the apex of the gynoecium. G, Whole plant phenotypes of *slk1*, *seu*, and *seu slk1*. Bar = 10 cm. H to M, Cleared ovules of the indicated genotypes. The extent of outer integument development is indicated with arrowheads. The majority (67%) of *seu* mutant ovules (H; Table III) display a wild-type extent of outer integument development (arrowhead). A minority (33%) of *seu* mutant ovules display a reduction in outer integument development (I; Table III). J shows enhanced ovule defects in the *seu slk1* double mutant. In K, the *slk1 slk2* double mutant appears morphologically wild type. In L and M, the disruption of ovule development is enhanced in *seu/+ slk1 slk2* gynoecia (M) relative to *seu/+ slk1* gynoecia (L). [See online article for color version of this figure.]

cial apex (Fig. 2, E and F, arrows). This short-valve phenotype is less penetrant in the first 10 flowers to arise from the inflorescence meristem and was observed in 6% of the carpels from these early-arising flowers. The short-valve phenotype and the loss of floral organs is reminiscent of similar phenotypes correlated with auxin homeostasis defects in the *ett*, *short valve1*, *pinoid*, *pin-formed1*, and *monopteros* (*mp*) mutants (Okada et al., 1991; Bennett et al., 1995; Sessions and Zambryski, 1995; Przemeck et al., 1996; Nishimura et al., 2005). These phenotypic enhancements were observed in both the *seu-3 slk1-1* and *seu-3 slk1-2* genotypes and similar but weaker enhancements were observed in the *seu-3 slk1-3* genotype, suggesting that *slk1-3* is an intermediate strength loss-of-function allele (data not shown).

SLK1 and *SLK2* Function in Ovule Outer Integument Development

To determine if *SLK1* functions during ovule development, we examined ovule development in the *seu*, *slk1*, and *seu slk1* genotypes. The *slk1* mutant plants display morphologically normal ovules and female gametophytes (Fig. 2K; data not shown). The *seu* single mutant displays a partially penetrant disruption of ovule development in which the outer integument fails to properly surround the nucellus and inner integument (Franks et al., 2002; Fig. 2, H and I). As a semiquantitative measure of outer integument growth, we determined the number of ovules that displayed wild-type outer integument development (i.e. greater than 90% coverage) as well as the number

Table II. *Floral organ counts for seu and slk mutants*

Genotype	Whorl 1	Whorl 2	Whorl 3	Whorl 4
Col-0 (n = 33)	4.0 (±0.0)	4.0 (±0.0)	5.9 (±0.24)	2.0 (±0.0)
slk1-1 (n = 33)	4.0 (±0.0)	4.0 (±0.0)	5.9 (±0.38)	2.0 (±0.0)
seu-3 (n = 30)	4.0 (±0.0)	4.0 (±0.0)	6.0 (±0.18)	2.0 (±0.0)
seu-3 slk1-1 (n = 49)	4.0 (±0.43)	2.2 (±1.1)	4.2 (±1.2)	1.4 (±0.54)

that displayed an intermediate disruption (between 90% and 50% coverage) or a severe disruption (less than 50% coverage) of outer integument development (Table III). In wild-type (ecotype Columbia [Col-0]) siliques, 100% of the ovules displayed wild-type outer integument development. In the *seu* mutant plants, 67% displayed wild-type outer integument development, while in the *seu slk1* double mutant, only 8% displayed wild-type development. Thus, the disruption of outer integument development was enhanced in the *seu slk1* double mutant relative to either single mutant (Fig. 2J).

Female gametophyte development in the *slk1* mutants did not deviate from that of the wild type (Table III). However, the *seu* mutants displayed a partially penetrant (18%) disruption of female gametophyte development. The female gametophytes in these ovules displayed a range of developmental abnormalities including missing, arrested, and morphologically abnormal female gametophytes. The *seu slk1* double mutant plants displayed an enhanced frequency of female gametophyte disruption (greater than 90%) relative to the *seu* single (Fig. 2J; Table III). As segregation ratios of progeny were not distorted from the predicted Mendelian values, the loss of the female gametophyte is likely due to an indirect effect of the maternal (sporophytic) tissues and not a haploinsufficiency during female gametophyte development (data not shown). To further investigate this, we examined ovules from *seu-3/+* and *slk1-1 seu-3/+* and found that the morphology of the female gametophyte was indistinguishable from that of the wild type (Table III). Examination of later developmental stages revealed normal endosperm and embryonic development. These results indicate that the *seu* and *seu slk1* chromosomes can be passed efficiently through the female gametophyte.

We also examined the role of *SLK2* during ovule development. Ovule development in the *slk2* single mutant and the *slk1 slk2* double mutant appeared morphologically normal (Fig. 2K; Table III). We could not examine *seu slk2* double mutant ovules because this genotype fails to make gynoecia (see below). However, *seu-3/+ slk1 slk2* plants displayed an enhanced disruption of the female gametophyte development and outer integument growth relative to the *seu-3/+ slk1* mutants (Table III; Fig. 2, L and M). Similarly, *seu-3 slk1/+ slk2/+* plants displayed enhanced ovule development disruptions relative to *seu-3 slk1/+* (Table III). These results indicate that *SLK2* functions during outer integument development, at least when *SEU* and *SLK1* activities are compromised.

SLK2 Shares Redundant Functions with *SEU* in the Early Embryo

In order to determine if *SLK2* shares redundant function with *SEU* during other stages of Arabidopsis development, we attempted to generate *seu slk2* double mutant plants. We examined the progeny of a self-cross from the parental genotype of *seu/+ slk2* and *seu/+ slk2/+* by planting seeds directly to soil. When using the strong *slk2-1* allele (a near RNA null), we were unable to recover *seu slk2-1* double mutant plants even after several hundred seeds were planted on soil. When the intermediate strength *slk2-2* allele was examined, we did recover *seu slk2-2* double mutant plants from *slk2-2/+ seu-3/+* parents, but these represented just 2% (three of 149) of the progeny, less than the 6.25% expected. These plants were very late

Table III. *Outer integument and female gametophyte defects in seu and slk mutant ovules*

Genotype	Percentage with Disrupted Female Gametophyte Development	Outer Integument Near Wild Type > 90%	Outer Integument Intermediate Disruption > 50%	Outer Integument Severe Disruption < 50%	*n*
Col-0	0	100	0	0	*n* = 76
seu-3/+	0	100	0	0	*n* = 97
seu-3	18	67	32	1	*n* = 87
slk1-1	0	100	0	0	*n* = 125
slk1-2	2	100	0	0	*n* = 43
slk2-1	0	100	0	0	*n* = 94
slk3-1	2	97	3	0	*n* = 111
slk1-1 slk2-1	0	100	0	0	*n* = 136
seu-3 slk1-1	94	8	60	32	*n* = 50
seu-3 slk1-2	44	9	86	5	*n* = 270
seu-3 slk-1–1/+	37	16	75	9	*n* = 105
seu-3 slk1-1/+ slk2-1/+	77	1	53	46	*n* = 104
seu-3/+ slk1-1	0	90	10	0	*n* = 59
seu-3/+ slk1-1 slk2-1	81	17	81	2	*n* = 268
seu-3/+ slk2-1	2	98	2	0	*n* = 44
lug-1	7	91	9	0	*n* = 395
slk1-1 lug-1	74	91	9	0	*n* = 350
lug-1 slk2-1	73	24	69	6	*n* = 62
slk1-1 lug-1 slk2-1	93	5	49	45	*n* = 226

flowering, they were very reduced in stature, and they exhibited severe floral phenotypes (Fig. 3; data not shown). The floral phenotypes were characterized by a reduction in floral organ number and a striking loss of the fourth whorl gynoecium. In these flowers, the fourth whorl was replaced by a small mound of morphologically indistinct tissue (Fig. 3A, arrowhead). In early-arising flowers from the *seu slk2-2* double mutants, the whorl 1 organs were narrow sepals (Fig. 3A). However, in late-arising flowers, the whorl 1 organs were carpelloid but failed to develop ectopic ovules (Fig. 3B, arrowhead). The *seu slk2-2* carpelloid whorl 1 organs and the overall floral phenotype are morphologically very similar to the previously described *seu lug* double mutant flowers (Franks et al., 2002).

The reduced segregation of the *seu slk2* double mutants suggested that seedling or embryonic lethality might be conditioned in the *seu slk2* double mutant. To examine seedling phenotypes, we planted seeds from the *seu*/+ *slk2-1* and *seu*/+ *slk2-2* parents onto Murashige and Skoog (MS) agar plates. In both of these populations, we observed a subset of seedlings that displayed a mutant phenotype. This phenotype was characterized by the development of narrow and small cotyledons (Fig. 3D). We genotyped a subset of morphologically abnormal seedlings and determined that all were *seu slk2* double mutants (11 of 11) using appropriate PCR-based markers (Supplemental Table S2). The extent of vascularization in the *seu slk2* cotyledons was dramatically reduced most often to a single centrally located vascular element (Fig. 3G). In sectioned material, the cotyledon mesophyll cells were larger in the *seu slk2* double mutant relative to the wild type, indicating that the reduction of cotyledon size was likely due to a reduction in cell number and not to a reduced cell size (Supplemental Fig. S4). In the majority of the *seu slk2* cotyledons examined, the morphology of the mesophyll cells and the vascular elements indicated that patterning along the adaxial/abaxial axis was relatively unaltered. However, in about 30% of the cotyledons examined, intermediate

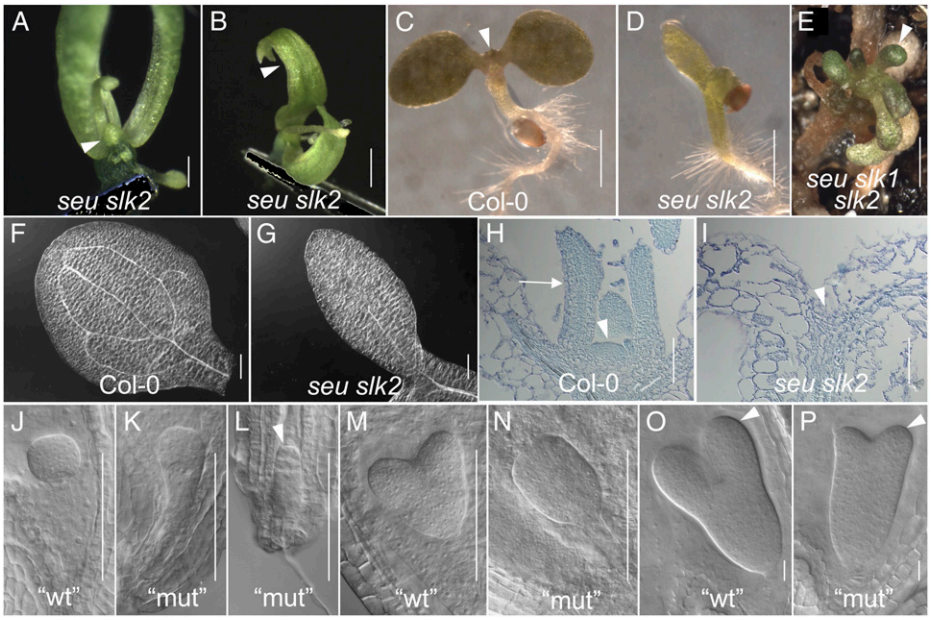

Figure 3. Floral, seedling, and embryonic phenotypes of *seu slk2* double mutants. A, Early-arising flower from *seu slk2* "escaper" plant. The arrowhead indicates a reduced gynoecial mound in whorl 4. B, Late-arising flower from *seu slk2* escaper plant. The arrowhead indicates carpelloid whorl 1 sepals. C to H, Seedlings at 5 d post germination. C, Wild-type (Col-0) seedling. The arrowhead indicates leaves initiating from the SAM. D, The *seu slk2* double mutant displays narrow cotyledons and a lack of true leaf development. E, A *seu slk1 slk2* triple mutant seedling that has escaped embryonic lethality displays bulbous and very reduced rosette leaves (arrowhead). F, Cleared wild-type (Col-0) cotyledon shows vascular loops. G, The *seu slk2* double mutant displays a very narrow cotyledon with a single unbranched central vascular element. H, Longitudinal section of a Col-0 seedling. SAM (arrowhead) and rosette leaf (arrow) are indicated. I, SAM and rosette leaves are not detected in the *seu slk2* seedling. The arrowhead indicates the expected location of the SAM if wild type. J to P, Embryos segregating from a *slk2/slk2 seu*/+ parental self-cross. Embryos were classified as morphologically wild type (wt) or mutant (mut). See text for details. J to L, Globular-stage sibling embryos displayed wild-type (J), weakly disrupted (K), or severely disrupted (L) morphologies. The arrowhead in L indicates a globular domain with reduced cell number. M and N, Heart-stage embryos. While cotyledon primordia are apparent in morphologically wild-type embryos (M), morphologically mutant sibling embryos (N) lack obvious cotyledon primordia. O and P, Reduced cotyledon development (arrowhead) is apparent at the torpedo stage in those embryos displaying mutant morphologies (compare P with O). Bars = 100 μm in A, E, F to I, and J to N, 200 μm in B, 1 mm in C and D, and 10 μm in O and P. [See online article for color version of this figure.]

or severe disruptions of adaxial/abaxial patterning were observed. In extreme cases, the cotyledons were radialized, lacked a morphologically distinct adaxial palisade layer, and displayed abnormal arrangements of vascular bundles (Supplemental Fig. S4). All *seu slk2* seedlings we examined lacked true leaves and the SAM. We examined chloral hydrate-cleared seedlings and toluidine blue-stained seedling sections and could not detect any morphological manifestation of the SAM or true leaves in the *seu slk2* double mutant seedlings (Fig. 3I). The *seu slk2* mutants displayed slightly shorter roots at 5 d post germination but appeared normal on a gross morphological level (data not shown). The *seu slk2* double mutant seedling phenotype is expected in 25% of the progeny; it was observed in 24% of the progeny from a self-cross of *seu*/+ *slk2-2* ($n = 457$) and 19% of the *seu*/+ *slk2-1* self-cross progeny ($n = 216$).

To look for defects during embryonic development, we examined siliques (seed pods) from *seu*/+ *slk2-2* parents. We observed deviations from the wild-type patterns of embryonic development in a subset of the embryos. The earliest defect that we identified was observed in three of 28 (11%) of the globular-stage embryos. We expect that 25% of the embryos in these siliques will be homozygous *slk2 seu* double mutants, suggesting that this early phenotype may not be fully penetrant. This globular-stage phenotype varied in its severity from mild to severe. Mild disruptions were characterized by fewer cells in the globular domain when compared with the wild type and less clearly organized tiers of cells (Fig. 3K). Severe disruptions displayed very few cells in the globular domain (eight cells in Fig. 3L, arrowhead) and some irregularity in the development of the suspensor. We also observed mutant phenotypes in 14 of 59 (24%) heart-stage embryos (Fig. 3N) and in torpedo-stage embryos (Fig. 3P) that were characterized by much smaller cotyledon primordia. While this paper was under review, Stahle et al. (2009) independently reported similar phenotypes in *seu slk2* double mutant seedlings and embryos.

SLK1 Function in Embryo and Seedling Development Is Revealed When *SLK2* and *SEU* Activity Is Compromised

We also examined seedling phenotypes in progeny from a *seu-3*/+ *slk1 slk2-1*/+ self-cross. From 473 seeds plated to MS plates, we recovered 66 seedlings (14%) that displayed narrow cotyledons and a reduction of the SAM. These seedlings were phenotypically similar to the *seu slk2* double mutant seedlings, but the majority of these had a less severe SAM phenotype. PCR analysis indicated that these seedlings were divided into two genotypes: *seu slk1 slk2-1*/+ and *seu slk1 slk2* triple mutant seedlings. The *seu slk1 slk2* triple mutant seedlings did survive for some time but remained very small. They produced few very small bulbous rosette leaves and appeared to be mostly lacking a clearly organized SAM (Fig. 3E). They accounted for less than 2% of the progeny (expected, 6.25%); thus, it is likely that the *seu slk1 slk2* triple mutant also conditions an embryonic lethality in the majority of instances and that these seedlings represent escapers that occasionally successfully complete embryogenesis and appear as severely disrupted seedlings. The *seu slk1 slk2-1*/+ seedlings were found at the approximately expected frequency of 12%, and these plants grew weakly and slowly, were late flowering, and displayed flowers that were similar to those of the *seu slk2* escaper plants (data not shown). These results support a role for *SLK1* during embryo or seedling development that is uncovered as *SEU* and *SLK2* activity is reduced.

SLK1 and *SLK2* Are Required with *ANT* and *SEU* for Ovule Initiation from the CMM

We sought to determine if *SLK* genes functioned during CMM development. As a measure of CMM function, we determined the number of ovule primordia that initiated in gynoecia of different genotypes. The *slk1* and *slk2* single mutants did not show a reduction in the number of ovules initiated from the CMM. The *slk1 slk2* double mutants showed a slight but statistically significant reduction in the number of ovules (89% of the wild type). As mutations in *SEU* enhance the loss of ovule primordia in *ant* mutants (Azhakanandam et al., 2008), we sought to determine if the *slk* mutants also enhanced the loss of ovules in the *ant* mutant background. The *ant-1* single mutant initiates only 64% of the wild-type number of ovule primordia (Table IV). In the *slk1 ant* and *ant slk2* double mutants, the numbers of initiated ovules fell further, to 41% and 47%, respectively. Finally, the *slk1 ant slk2* triple mutants generated only 19% of the wild-type ovule number. We then generated *seu*/+ *slk1 ant slk2* mutant plants and observed a complete absence of ovule primordia in these gynoecia (Table IV; Fig. 4K).

Decreasing the activity of *SEU* and the *SLK* genes in the *ant* mutant background also had additional effects on the overall development of the gynoecium and other tissues derived from the CMM. The *slk1 slk2* (Fig.

Table IV. *Ovule primordia counts from mature gynoecia*

Organ	Col-0	*slk1 slk2*	*ant*	*slk1 ant*	*ant slk2*	*slk1 ant slk2*	*seu*/+ *slk1 ant slk2*
Ovule primordia	47 ± 3.7 ($n = 24$)	42 ± 3.2 ($n = 24$)	30 ± 1.6 ($n = 25$)	20 ± 4.1 ($n = 25$)	22 ± 5.3 ($n = 24$)	9 ± 6.0 ($n = 24$)	0 ± 0.0 ($n = 16$)
Ovules (% of wild type)	100	89	64	43	47	19	0

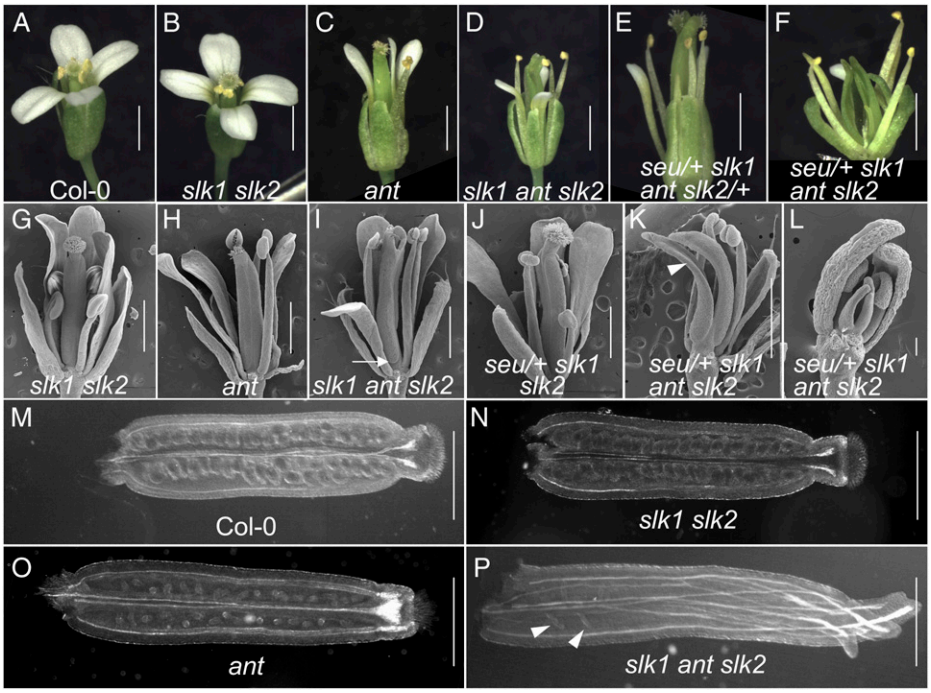

Figure 4. *SLK1* and *SLK2* are required with *ANT* and *SEU* for ovule initiation from the CMM. A, Col-0 flower. B, Morphology of a *slk1 slk2* mutant flower is near that of Col-0. C, *ant* mutant. D, Gynoecial disruptions are enhanced in *slk1 ant slk2* triple mutant relative to the *ant* and *slk1 slk2* mutants. E and F, More severe reductions of CMM-derived tissues are observed in *seu/+ slk1 ant slk2* (F) relative to the *seu/+ slk1 ant slk2/+* (E) genotype. G to L, Scanning electron micrographs of flowers from the indicated genotypes. In I, the arrow indicates the basal valve boundary. In K, the *seu/+ slk1 ant slk2* genotype conditions complete loss of ovule primordia and severe reduction of CMM-derived tissues (arrowhead). L shows a stage 10 flower. Disruption of the CMM is already evident at this stage. M to P, Optical cross sections from cleared gynoecia of the indicated genotypes. Arrowheads in P indicate the few ovules that have initiated. Bars = 1 mm in A to K, 100 μm in L, and 0.5 mm in M to P. [See online article for color version of this figure.]

4, B and G) and *ant* (Fig. 4, C and H) genotypes displayed nearly wild-type external gynoecial morphology. The *ant* single mutants displayed a slight reduction in stigmatic tissue and occasionally very slight splitting of the gynoecial apex (Fig. 4, C and H; Elliott et al., 1996; Klucher et al., 1996). The *slk1 ant slk2* genotype conditioned an increased carpel splitting and a nearly complete loss of stigmatic tissue (Fig. 4, D and I). The basal valve boundary was often shifted apically on one or both valves of the gynoecial tube (Fig. 4I, arrow). Occasionally, trichome-like cells were observed at the apex of the *slk1 ant slk2* mutant gynoecia (data not shown). These arose from the style-like cells that were present at the tips of the individual carpels. The *seu/+ slk1 ant slk2* genotype was severely inhibited in its ability to form CMM tissues (Fig. 4, K and L). In addition to the complete loss of ovule primordia (Table IV), the gynoecia were dramatically split and stigmatic, stylar, and septal tissues were almost completely absent (Fig. 4K). In comparison with the *seu/+ slk1 ant slk2* gynoecia, *seu/+ slk1 slk2* gynoecia (Fig. 4J) exhibited a less severe disruption of overall gynoecial morphology that was characterized by a fused gynoecial tube topped by an extended stylar region and wild-type amounts of stigmatic tissue. These data together suggest that *slk1* and *slk2* play a partially redundant role with *seu* and *ant* during CMM and gynoecial development.

Mutations in *slk1* and *slk2* Enhance *lug* Ovule and Floral Defects

Mutations in *SEU* dramatically enhance the *lug* mutant phenotype and result in enhanced *AG* derepression and associated homeotic organ transformations, enhanced floral organ loss, and severe reductions of the gynoecial mound (Franks et al., 2002). In order to determine if mutations in the *SLK* genes enhanced the *lug* phenotype, we created a series of higher order mutant combinations employing the *lug-1* allele (Liu and Meyerowitz, 1995) that was first introgressed into the Col-0 background. The *lug-1* (Col-0) mutant flowers exhibit splitting of the gynoecium at the apex and slightly narrower floral organs relative to the wild type (Fig. 5E). However, homeotic transformations are only rarely observed in the Col-0 background. The loss of *slk1* and *slk2* in the *lug-1* (Col-0) mutant background conditioned relatively subtle enhancements relative to the *lug-1* (Col-0) single mutant. The most obvious of these was noted in ovules (Fig. 5; Table III). As *slk1* and *slk2* activity are reduced in the *lug-1* (Col-0) mutant background, the extent and

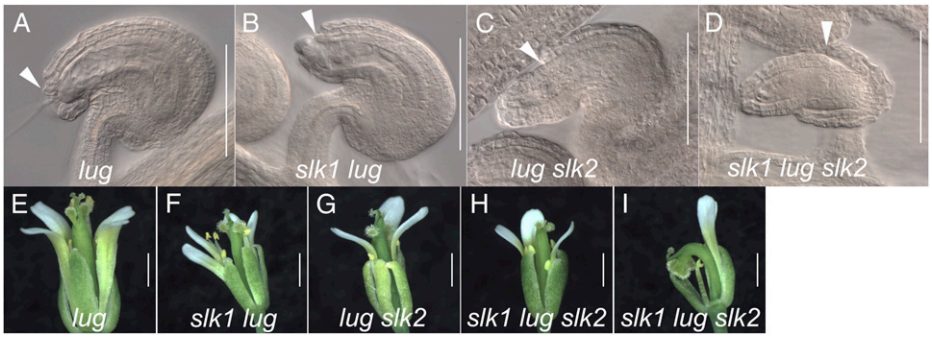

Figure 5. Mutations in *SLK1* and *SLK2* enhance the *lug* ovule and floral phenotypes. A to D, Cleared ovules from gynoecia of the indicated genotypes. Arrowheads indicate the extent of outer integument development. Bars = 100 μm. E to I, Floral phenotypes of the indicated genotypes. H and I show the two-carpel and one-carpel phenotypes observed in the *slk1 lug slk2* triple mutant flowers, respectively. The one-carpel gynoecia are often curved and bent over. Bars = 1 mm. [See online article for color version of this figure.]

penetrance of the ovule outer integument disruption is increased (Fig. 5, A–D). The *slk1 lug*, *lug slk2*, and *slk1 lug slk2* mutants also displayed slightly narrower sepals, reduced pollen development, and a smaller overall floral size than the *lug* single mutant (Fig. 5, E–I). The *lug slk2* and *slk1 lug slk2* mutants increased the percentage of gynoecia composed by a single carpel (Fig. 5I). However, none of the *slk1 lug slk2* higher mutant combinations conditioned severe homeotic transformations within the flower, nor did they condition severe gynoecial disruptions. This was somewhat surprising, given the severe reduction of gynoecium extent and the enhanced carpelloidy previously reported in the *seu lug* double mutant (Franks et al., 2002).

SLK2 Is Expressed in the CMM and Young Floral Organ Primordia

Evaluation of data available with the Genevestigator software tool suggests that the expression of the *SLK* genes is widespread throughout developmental stages

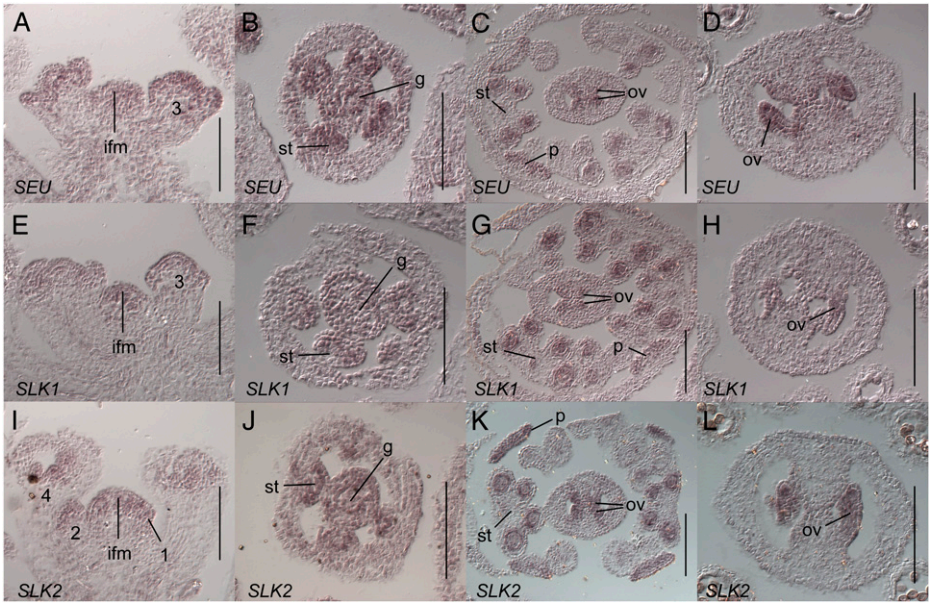

Figure 6. *SEU*, *SLK1*, and *SLK2* are expressed in young flower meristems, ovules, and the CMM. In situ hybridization on wild-type (Col-0) tissue with a *SEU* (A–D), *SLK1* (E–H), or *SLK2* (I–L) antisense probe (A–E and G–H). A, E, and I, Inflorescence longitudinal sections. Hybridization signal is detected in the inflorescence meristem (ifm) and throughout stage 1, 2, and early 3 floral primordia. Numbers indicate floral stages (Smyth et al., 1990). B, F, and J, Stage 6 floral cross section. Expression is detected throughout gynoecial mound (g) and stamen (st) primordia. C, G, and K, Stage 9 or early 10 floral cross sections. Expression is detected in ovules (ov) and petals (p). Within the stamens, expression is detected most strongly in the locules, pollen mother cells, and the tapetum. D, H, and L, Gynoecial cross sections show expression throughout the ovules at floral stages 10 or 11. Bars = 100 μm.

and tissues (Zimmermann et al., 2004; Grennan, 2006). These data support a general difference in the level of expression of the *SEU* and *SLK* mRNAs, with the relative levels of expression being *SEU* > *SLK2* > *SLK1* (Supplemental Fig. S1). Our qRT-PCR data from inflorescence tissue supported the expression of these three genes as well as *SLK3* in RNA prepared from inflorescence tissues (Supplemental Fig. S2).

To determine the tissue-specific expression patterns of *SEU*, *SLK1*, and *SLK2*, we employed in situ hybridization using specific antisense probes (see "Materials and Methods"). We carefully examined expression patterns in the inflorescence meristem through stage 12 flowers and found that the patterns of expression of *SEU*, *SLK1*, and *SLK2* were indistinguishable. However, the level of expression from the *SEU* probe was consistently higher than that of the *SLK2* probe, which was generally higher than *SLK1*. The detailed description below describes the expression patterns of all three genes examined. We detected strong signal in the inflorescence meristem and throughout young floral meristems at stages 1 through early 3 (Fig. 6, A, E, and I). Stages are according to Smyth et al. (1990). During late stage 3 and stage 4, signal is more strongly detected in the adaxial and marginal portions of the sepal primordia (data not shown). Expression is detected throughout the stamen anlagen/primordia at stage 4 and then becomes restricted to the developing tepetum and microspore mother cells (locules) during later stages (Fig. 6, C, G, and K). Expression within the petals is seen throughout the primordia as they arise (data not shown) and remains in the expanding blade through at least stage 10 (Fig. 6, C, G, and K). Expression is detected throughout the gynoecium at stages 6 and 7 (Fig. 6, B, F, and J). By stage 8, gynoecial expression is most highly detected within the CMM (medial ridge) and in the developing ovule anlagen and primordia (Fig. 6, C, G, and K). Expression is detected throughout the ovules until at least floral stage 11, corresponding to ovule stage 3-I according to Schneitz et al. (1995; Fig. 6, D, H, and L; data not shown). No signal was detected with a control sense strand probe, and signal with the antisense probes was greatly reduced in each respective mutant tissue (Supplemental Fig. S3), further confirming the specificity of the hybridization conditions and probes.

SEU and *SLK1* Are Required for Optimal Auxin Signaling during Root and Gynoecial Development

Work from Pfluger and Zambryski (2004) indicated that *SEU* is required for proper response to the plant phytohormone auxin. To determine if *SLK1* is required for the ability to respond to auxin, we examined expression from the auxin-responsive DR5:GUS reporter (Ulmasov et al., 1997) in Col-0, *slk1*, *seu*, and *seu slk1* seedling roots 7 d after germination. In Col-0 seedlings, GUS activity was observed strongly in the root tip and at intermediate levels in the stele (root vascular tissue; Fig. 7A). In the *slk1* single mutant roots, the activity of DR5:GUS reporter appeared reduced relative to the wild type (Fig. 7C). This is similar to the reduced expression of DR5:GUS in the *seu* single mutant (Pfluger and Zambryski, 2004; Fig. 7B). The DR5:GUS reporter activity was also reduced in the *seu slk1* double mutant relative to the wild type.

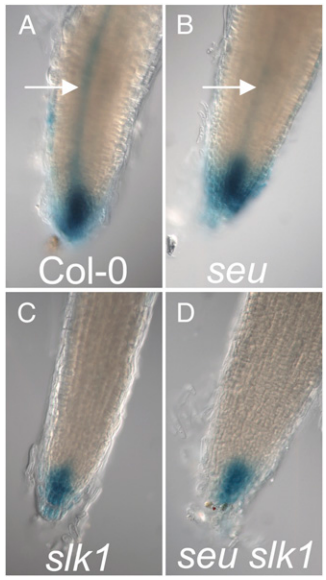

Figure 7. The *seu*, *slk1*, and *seu slk1* mutants display reduced DR5-GUS activity. DR5:GUS reporter activity is shown in primary root apices of the indicated genotypes. Arrows in A and B indicate stele (root vasculature). [See online article for color version of this figure.]

To determine if altered auxin signaling might contribute to the floral and gynoecial defects observed in the *seu slk1* double mutants, we examined the expression of genes with known auxin synthesis (*YUCCA4* [*YUC4*]) and auxin response (*ETT* and *MP*) functions as well as two genes known to be induced by auxin (*INDOLE ACETIC ACID1* [*IAA1*] and *IAA17*; Abel et al., 1994; Sessions et al., 1997; Hardtke and Berleth, 1998; Zhao et al., 2001). Although not directly tied to auxin regulation, we also examined levels of *PHB* and *REVOLUTA* (*REV*) mRNA, as reductions in *PHB* and *REV* expression have been reported in the *seu ant* double mutant carpels (Azhakanandam et al., 2008). We examined the expression of these genes in two different RNA samples: inflorescence apices (containing the inflorescence meristem and floral stages 1–6) and staged dissected gynoecia from floral stages 8 to 10 (Tables V and VI). We were particularly interested to identify genes in which the expression in the *seu slk1* double mutant was statistically different from each of the single mutants as well as the wild type. These genes might underlie the synergistic enhancement of phenotypes seen in the *seu slk1* double mutant. In the inflorescence apices samples, *IAA1*, *IAA17*, *MP*, *PHB*, and *REV* fell into this statistically significant category (Table V). The levels of *IAA1*, *IAA17*, *MP*, *PHB*, and *REV* expression in the *seu slk1* double mutant are reduced to 20%, 36%, 26%, 24%, and 43% of the wild-

Table V. *qRT-PCR quantification in inflorescence meristem through stage 6 flowers*

Late-arising flowers are flowers 20 to 35 from the apical meristem. ± values are SE.

Gene	Col-0	*slk1*	*seu*	*seu slk1*
IAA1	0.10 ± 0.01	0.07 ± 0.01	0.05 ± 0.01	0.02 ± 0.002[a,b]
IAA17	1.7 ± 0.0	1.1 ± 0.0	1.0 ± 0.0	0.62 ± 0.0[a,b]
YUC4	0.09 ± 0.01	0.24 ± 0.04	0.09 ± 0.02	0.07 ± 0.006
MP	13.5 ± 1.7	6.4 ± 0.46	6.7 ± 0.50	3.5 ± 0.31[a,b]
ETT	2.5 ± 0.48	2.1 ± 0.30	1.6 ± 0.03	0.98 ± 0.19[a]
PHB	0.96 ± 0.09	0.59 ± 0.05	0.50 ± 0.05	0.23 ± 0.02[a,b]
REV	2.8 ± 0.17	3.4 ± 0.12	1.9 ± 0.03	1.2 ± 0.08[a,b]

[a]Statistically different from Col-0 at $P < 0.05$. [b]Statistically different from all other genotypes at $P < 0.05$.

type level, respectively. The level of *YUC4* expression was not statistically different between these genotypes. The expression of *ETT* was significantly reduced in the *seu slk1* double mutant inflorescence apices relative to Col, but it was not statistically different from expression in the *seu* single mutant. In the dissected gynoecia (stages 8–10), we also detected a statistically significant reduction in expression of *MP* and *PHB* in the *seu slk1* mutants relative to the wild type and both single mutants. Expression levels were reduced to 35% and 21% of wild-type levels, respectively (Table VI).

We also used qRT-PCR to characterize gene expression in 6-d-old *seu slk2* double mutant seedlings. These experiments indicated that the levels of *STM* and *PHB* were reduced in the *seu slk2* mutant seedlings to 20% and 30% of wild-type levels, respectively (Table VII). The levels of expression in the *seu slk2* double mutants were statistically lower than in the wild type and all of the single mutants.

DISCUSSION

The *SEU*-related genes encode putative transcriptional adaptor proteins with sequence similarity to metazoan Ldb-type transcriptional adaptors. These transcriptional adaptors in both animals and plants function in many gene regulation events and are required for a diversity of developmental processes. In Arabidopsis, *SEU* functions with *LUG* in the repression of *AG* in perianth floral organs, with *ETT* for correct auxin response during floral organ patterning and with *ANT*, *LUG*, and *FIL* for the proper initiation of ovule primordia from the marginal domain of the carpel. Here, we demonstrate that *SLK1* and *SLK2* share a high degree of functional similarity to *SEU* during this diverse set of developmental events. However, our results also indicate that a degree of functional differentiation exists between the different members of the *SEU*-related gene family. We show that loss of *SLK* gene function leads to altered auxin responses, altered development of the CMM, but surprisingly little effect on floral organ identity specification. Additionally, we report a novel role for *SEU* and *SLK2* during embryonic SAM development.

Role of *SLK* Genes in Auxin Signaling

The *seu* single mutants exhibit reduced expression of the DR5:GUS auxin-responsive reporter (Pfluger and Zambryski, 2004). Additionally, SEU physically interacts with ETT/ARF3 in a yeast two-hybrid assay and thus may directly participate in the regulation of auxin-responsive genes (Pfluger and Zambryski, 2004). Here, we show that *slk1* and *seu slk1* mutants also display reduced levels of expression from the DR5:GUS reporter in the root. Furthermore, the *seu slk1* and *seu slk2* flowers display a number of phenotypes that have been reported in mutant plants for auxin synthesis, transport, or signaling components (Okada et al., 1991;

Table VI. *qRT-PCR quantification in stage 8 to 10 carpels*

Late-arising flowers are flowers 20 to 35 from the apical meristem. ± values are SE.

Gene	Col-0	*slk1*	*seu*	*seu slk1*
IAA1	0.06 ± 0.006	0.03 ± 0.001	0.02 ± 0.002	0.02 ± 0.0007[a]
IAA17	1.0 ± 0.11	0.55 ± 0.05	0.66 ± 0.04	0.56 ± 0.03[a]
YUC4	0.14 ± 0.015	0.25 ± 0.03	0.09 ± 0.005	0.07 ± 0.007[a]
MP	16.1 ± 1.0	11.8 ± 0.75	8.7 ± 0.81	5.6 ± 0.39[a,b]
ETT	2.85 ± 0.77	1.35 ± 0.11	0.92 ± 0.05	1.12 ± 0.04[a]
PHB	1.17 ± 0.18	0.76 ± 0.04	0.76 ± 0.11	0.25 ± 0.01[a,b]
REV	4.5 ± 0.68	3.2 ± 0.23	2.6 ± 0.25	1.6 ± 0.20[a]

[a]Statistically different from Col-0 at $P < 0.05$. [b]Statistically different from all other genotypes at $P < 0.05$.

Table VII. *qRT-PCR quantification in 6-d-old seedlings*

± values are SE.

Seedling	Col-0	*slk2-1*	*slk2-2*	*seu*	*seu slk2-1*	*seu slk2-2*	Statistical Significance Yes/No (*P*)
STM	$2.2 \times 10^{-4} \pm 2.6 \times 10^{-5}$	$2.0 \times 10^{-4} \pm 1.8 \times 10^{-5}$	$2.1 \times 10^{-4} \pm 8.5 \times 10^{-6}$	$3.2 \times 10^{-4} \pm 4.2 \times 10^{-5}$	$5.6 \times 10^{-5} \pm 6.3 \times 10^{-6}$	$4.4 \times 10^{-5} \pm 6.1 \times 10^{-6}$	Yes (0.0001)
PHB	0.33 ± 0.01	0.23 ± 0.005	0.31 ± 0.03	0.18 ± 0.01	0.11 ± 0.008	0.09 ± 0.005	Yes (0.004)

Bennett et al., 1995; Sessions and Zambryski, 1995; Przemeck et al., 1996; Friml et al., 2004; Nishimura et al., 2005; Cheng et al., 2006; Stepanova et al., 2008; Tao et al., 2008). These include shifts in the basal boundary of the gynoecial valve in *seu slk1* plants and reductions in floral organ number in both *seu slk1* and *seu slk2* flowers. These results suggest that some of the *seu slk1* and *seu slk2* defects may be conditioned by altered auxin response or homeostasis. In further support of this hypothesis, we identified two genes previously shown to be induced by auxin (*IAA1* and *IAA17*) and two genes with known roles in auxin signaling (*MP* and *ETT*) whose expression was reduced in *seu slk1* inflorescences. A reduced ability to respond to auxin maxima in the *seu slk1* and *seu slk2* double mutants might in part underlie the loss of floral organs, as these organ initiation events are known to be marked by auxin maxima and require functioning auxin pathways (Benkova et al., 2003). In the case of ETT, the *SEU*-related genes may regulate ETT activity at two levels: at the level of mRNA abundance (as supported by qRT-PCR data) and through direct protein-protein interactions, as have been shown for SEU and ETT (Pfluger and Zambryski, 2004).

SEU and *SLK* Genes May Support CMM and SAM Development by Similar Mechanisms

Our analysis of *SLK1* and *SLK2* suggests that these two genes function during the development of the marginal domain of the carpel and the initiation of ovule primordia from the CMM. Our in situ hybridization data indicate that *SEU*, *SLK1*, and *SLK2* are all expressed in the developing CMM and ovule primordia throughout their early development and thus likely function in a cell autonomous manner in these tissues. The *seu/+ slk1 ant slk2* mutant conditions a dramatic loss of ovule primordia that is similar to that previously reported for *seu ant* double mutants. Thus, it appears that within the CMM, *SLK1* and *SLK2* also support ovule initiation in a manner similar to that of *SEU*. However, the fact that single mutations in *seu*, *slk1*, and *slk2* all independently enhance the phenotypes of *ant* mutants suggests that either the *SEU*-related genes are not completely substitutable during CMM development or that the initiation of ovules in the *ant* mutant responds to activities of the *SEU*-related genes in a graded fashion.

Within the *seu ant* CMM, the loss of ovule primordia has been correlated with a loss of *PHB* expression within the developing core of the gynoecium (Azhakanandam et al., 2008). Here, we report a reduction of *PHB* mRNA levels in *seu slk2* mutant seedlings. We speculate that the CMM and SAM defects are mechanistically related to this reduction in *PHB* expression. Additionally, we report a reduction of *STM* levels in the *seu slk2* seedlings. *STM* is known to play a key role in the maintenance of meristematic properties in both the SAM and the CMM (Long et al., 1996; Scofield et al., 2007). By supporting the expression of *PHB* and *STM*, *SEU* and *SLK* genes may function to maintain meristematic potential in both the CMM and the SAM. As *PHB* and *STM* expression is not known to be directly responsive to auxin and meristematic regions are typically maintained by lower auxin-cytokinin ratios (Shani et al., 2006), we suggest that the mainte-

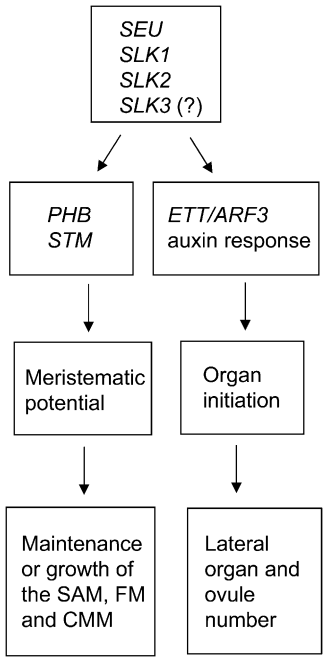

Figure 8. Model of functional roles of *SEU* and *SLK* genes in the SAM and CMM. In this model, we propose that the *SEU*, *SLK1*, *SLK2*, and possibly *SLK3* genes support the development of organs from the SAM, the floral meristem (FM), and the CMM through two gene regulatory events (right and left sides). *SEU* and the *SLK* genes support auxin responses that are required for organ initiation events in the CMM, floral meristem, and embryonic SAM. Additionally, *SEU* and *SLK* genes support the maintenance or growth of these meristematic regions by enabling the expression of *PHB* and *STM*.

nance of meristematic potential that is supported by *SEU*, *SLK1*, and *SLK2* is not due to their role in auxin response. Rather, we propose a model in which *SEU* and *SLK* genes support meristematic properties by potentiating the expression of *PHB* and *STM* either directly or indirectly in a manner independent from the abovementioned role of *SEU* and *SLK* in the auxin response. We suggest that the dramatic loss of ovule primordia that is conditioned in the *seu ant* (Azhakanandam et al., 2008) and *seu/+ slk1 ant slk2* mutants (Fig. 4; Table IV) is the result of a reduction in gynoecial meristematic potential coincident with a reduced auxin response in ovule anlagen during their earliest stages of initiation (Fig. 8). This results in a complete loss of ovule primordia as well as a reduction in other tissues derived from the CMM/medial ridge in these genotypes.

Functional Redundancy and Diversification within the *SEU*-Related Gene Family

The *slk1 slk2* double mutant and the *seu* single mutant both progress through embryogenesis without noticeable defects. However, the concomitant loss of both *SLK2* and *SEU* conditions a severe embryonic defect in SAM and cotyledon development. Thus, during embryonic development, *SEU* and *SLK2* appear to be functionally interchangeable and provide an important redundant function supporting embryonic SAM development. Our data indicate that *SLK1* and *SLK3* cannot provide a sufficient level of this activity to support embryonic SAM development, at least when expressed from their endogenous promoters in the *seu slk2* double mutant background. Further characterization of expression patterns as well as ectopic expression or domain-swap constructs may help to elucidate the molecular mechanisms that underlie the functional diversity within the *SEU*-related genes. Interestingly, the *lug luh* double mutant genotype also conditions an embryonic lethality (Sitaraman et al., 2008). However, the degree of similarity between the molecular causes of the *lug luh* and *seu slk2* embryonic defects remains to be determined.

Mechanism of Functional Redundancy within the *SEU*-Related Gene Family

In the developmental events that we have analyzed, members of the *SEU*-related gene family often share some degree of functional redundancy. One mechanistic explanation for this redundancy would be an overlap in the physical partners of the *SEU*-related proteins. SEU has been shown to work in complexes with several MADS domain proteins and with ETT, LUG, and LUH. It will be interesting to determine if the SLK proteins can also interact with these proteins. All three *SLK* genes appear to encode an LCCD, suggesting that they form physical complexes with either LUG or LUH proteins. Also supporting this proposition, SLK homologs in *Antirrhinum* can physically interact with the LUG *Antirrhinum* ortholog STYLOSA (Navarro et al., 2004), and recently, LUG and LUH have been reported to interact with Arabidopsis SLK proteins in a yeast two-hybrid assay (Stahle et al., 2009). An alternative, but not mutually exclusive, possibility is that SEU and SLK proteins form heterodimeric complexes. The conserved DD in the metazoan Ldb proteins mediates dimerization events that are required for the formation of higher order protein complexes (Agulnick et al., 1996; Jurata et al., 1996; Jurata and Gill, 1997; Morcillo et al., 1997). This domain may function similarly in the SEU and SLK proteins in Arabidopsis and mediate either homodimeric or heterodimeric interactions. Heterodimeric complexes between SEU and SLK proteins would provide a mechanism through which the SLK proteins could modulate the activity of transcriptional complexes that contain SEU. Furthermore, as the protein sequences of the SEU protein and the SLK proteins diverge outside of the central DD and LCCD, heterodimeric SEU/SLK complexes would likely contribute a more diverse protein interaction surface than homodimeric forms, allowing the *SEU*-related gene family to participate in a wider diversity of gene regulation events.

Role of *SLK* Genes in the Repression of *AG*

It is notable that *slk1* and *slk2* mutants only mildly enhance the floral phenotypes of the *lug* single mutant. We did not observe enhanced homeotic organ identity transformations, as has been reported for the *seu lug* and *luh/+ lug* mutants (Franks et al., 2002; Sitaraman et al., 2008). Additionally, the *seu slk1*, *slk1 slk2*, and *seu slk2* double mutants rarely displayed carpelloidy that would indicate ectopic *AG* expression within the floral meristem. Only in late-arising *seu slk2* and rarely in *seu slk1* flowers were carpelloid whorl 1 organs observed. These results might be explained by *SLK3* activity still present in these plants. Alternatively, these results may suggest that *SLK1* and *SLK2* play a lesser role in the repression of *AG* than does *SEU*. This may reflect a differential ability of SEU and SLK proteins to physically interact with LUG or other regulators in the flower.

MATERIALS AND METHODS

Mutant Alleles

The Arabidopsis (*Arabidopsis thaliana*) alleles of *SLK* genes used in this study are reported in Supplemental Table S1. We amplified and sequenced the DNA junction fragment using the appropriate border primers (Supplemental Table S2) to confirm each insertion site. Each mutant line was backcrossed to the parent ecotype three times before generating homozygous stocks for phenotypic and genetic analysis. The *seu-3* and *ant-1* alleles have been reported previously (Klucher et al., 1996; Pfluger and Zambryski, 2004). The *lug-1* allele was originally isolated in the Landsberg *erecta* ecotype (Liu and Meyerowitz, 1995) and has subsequently been backcrossed into Col-0 for four generations before use in this study. Upon request, all novel materials described in this publication will be made available in a timely manner for noncommercial research purposes, subject to the requisite permission from any third-party owners of all or parts of the material. Obtaining any permissions will be the responsibility of the requestor.

Phylogenic Analysis

ClustalW2 (http://www.ebi.ac.uk/Tools/clustalw2/index.html) was used to align amino acid sequences of the full-length proteins. The optimal tree with the sum of branch length = 4.91935227 was inferred using the neighbor-joining method (Saitou and Nei, 1987). The percentage of replicate trees in which the associated taxa clustered together in the bootstrap test (1,000 replicates) is shown next to the branches (Felsenstein, 1985). The tree is drawn to scale, with branch lengths in the same units as those of the evolutionary distances used to infer the phylogenetic tree. The evolutionary distances were computed using the Poisson correction method (Zuckerkandl and Pauling, 1965) and are in units of the number of amino acid substitutions per site. All positions containing alignment gaps and missing data were eliminated only in pairwise sequence comparisons (pairwise deletion option). There were a total of 1,232 positions in the final data set. Phylogenetic analyses were conducted in MEGA4 (Tamura et al., 2007). Protein sequence identity and similarity matrix was calculated with the Matrix Global Alignment tool (Campanella et al., 2003).

In Situ Hybridization and Microscopy

In situ hybridizations were carried out as reported previously (Franks et al., 2002) with the following modifications: acetic anhydride and RNase treatment steps were omitted. A detailed protocol is available at http://www4.ncsu.edu/~rgfranks/research/protocols.html. The *SEU*, *SLK1*, and *SLK2* antisense probes were generated from pCRII_SEU_HFFL and Arabidopsis Biological Resource Center clones G66746 and G10219, respectively. Probes were made corresponding to the C-terminal domains and did not overlap highly conserved DD/LCCD regions. Scanning electron and light microscopy were performed as described previously (Azhakanandam et al., 2008).

qRT-PCR Analysis and GUS Analysis

qRT-PCR analysis was as described previously (Azhakanandam et al., 2008). Results shown in Tables V, VI, and VII are mean expression of the indicated gene normalized relative to *ADENOSINE PHOSPHORIBOSYL TRANSFERASE* (AT1G27450). Results are averages and SE of the mean from three technical replicates of three biological replicates. Statistical analysis was done in JMP 7.0 (SAS Institute). Statistical differences of means were evaluated by pairwise *t* tests in all combinations. For GUS analysis, seedlings were grown on half-strength MS + 10% Suc under 16-h/8-h light/dark conditions and assayed 7 d after germination. For photography, seedlings were stained for either 2 or 4 h at room temperature and then cleared in 70% ethanol.

Supplemental Data

The following materials are available in the online version of this article.

Supplemental Figure S1. Genevestigator expression data for *SEU* and *SLK* genes.

Supplemental Figure S2. qRT-PCR expression data for *SLK1*, *SLK2*, and *SLK3* in *slk1* and *slk2* mutant inflorescences.

Supplemental Figure S3. Specificity of the *SEU*, *SLK1*, and *SLK2* antisense in situ probes.

Supplemental Figure S4. Morphological alterations of cotyledon mesophyll cells and vascular elements in the *seu slk2* double mutant.

Supplemental Table S1. Alleles of *SLK* transcriptional coregulators in Arabidopsis.

Supplemental Table S2. Oligonucleotides used in this study.

Supplemental Table S3. qRT-PCR quantification in inflorescence meristem through stage 6 flowers (from early-arising flowers).

Supplemental Table S4. qRT-PCR quantification in stage 8 to 10 carpels (from early-arising flowers).

ACKNOWLEDGMENTS

We thank L. Mathies, A. Stepanova, and the anonymous reviewers for comments on the manuscript; the Arabidopsis Biological Resource Center for the distribution of mutant seed stocks; and the North Carolina State University Center for Electron Microscopy and Cellular and Molecular Imaging.

Received August 13, 2009; accepted December 4, 2009; published December 9, 2009.

LITERATURE CITED

Abel S, Oeller PW, Theologis A (1994) Early auxin-induced genes encode short-lived nuclear proteins. Proc Natl Acad Sci USA **91:** 326–330

Agulnick AD, Taira M, Breen JJ, Tanaka T, Dawid IB, Westphal H (1996) Interactions of the LIM-domain-binding factor Ldb1 with LIM homeodomain proteins. Nature **384:** 270–272

Alonso JM, Stepanova AN, Leisse TJ, Kim CJ, Chen H, Shinn P, Stevenson DK, Zimmerman J, Barajas P, Cheuk R, et al (2003) Genome-wide insertional mutagenesis of *Arabidopsis thaliana*. Science **301:** 653–657

Azhakanandam S, Nole-Wilson S, Bao F, Franks RG (2008) SEUSS and AINTEGUMENTA mediate patterning and ovule initiation during gynoecium medial domain development. Plant Physiol **146:** 1165–1181

Benkova E, Michniewicz M, Sauer M, Teichmann T, Seifertova D, Jurgens G, Friml J (2003) Local, efflux-dependent auxin gradients as a common module for plant organ formation. Cell **115:** 591–602

Bennett SRM, Alvarez J, Bossinger G, Smyth DR (1995) Morphogenesis in pinoid mutants of Arabidopsis thaliana. Plant J **8:** 505–520

Bowman JL, Baum SF, Eshed Y, Putterill J, Alvarez J (1999) Molecular genetics of gynoecium development in *Arabidopsis*. Curr Top Dev Biol **45:** 155–205

Campanella JJ, Bitincka L, Smalley J (2003) MatGAT: an application that generates similarity/identity matrices using protein or DNA sequences. BMC Bioinformatics **4:** 29

Cheng Y, Dai X, Zhao Y (2006) Auxin biosynthesis by the YUCCA flavin monooxygenases controls the formation of floral organs and vascular tissues in Arabidopsis. Genes Dev **20:** 1790–1799

Conner J, Liu Z (2000) *LEUNIG*, a putative transcriptional corepressor that regulates *AGAMOUS* expression during flower development. Proc Natl Acad Sci USA **97:** 12902–12907

Curtis MJ, Belcram K, Bollmann SR, Tominey CM, Hoffman PD, Mercier R, Hays JB (2009) Reciprocal chromosome translocation associated with TDNA-insertion mutation in Arabidopsis: genetic and cytological analyses of consequences for gametophyte development and for construction of doubly mutant lines. Planta **229:** 731–745

Elliott RC, Betzner AS, Huttner E, Oakes MP, Tucker WQ, Gerentes D, Perez P, Smyth DR (1996) *AINTEGUMENTA*, an *APETALA2*-like gene of *Arabidopsis* with pleiotropic roles in ovule development and floral organ growth. Plant Cell **8:** 155–168

Felsenstein J (1985) Confidence limits on phylogenies: an approach using the bootstrap. Evolution **39:** 783–791

Franks RG, Wang C, Levin JZ, Liu Z (2002) *SEUSS*, a member of a novel family of plant regulatory proteins, represses floral homeotic gene expression with *LEUNIG*. Development **129:** 253–263

Friml J, Yang X, Michniewicz M, Weijers D, Quint A, Tietz O, Benjamins R, Ouwerkerk PB, Ljung K, Sandberg G, et al (2004) A PINOID-dependent binary switch in apical-basal PIN polar targeting directs auxin efflux. Science **306:** 862–865

Gonzalez D, Bowen AJ, Carroll TS, Conlan RS (2007) The transcription corepressor LEUNIG interacts with the histone deacetylase HDA19 and mediator components MED14 (SWP) and CDK8 (HEN3) to repress transcription. Mol Cell Biol **27:** 5306–5315

Gregis V, Sessa A, Colombo L, Kater MM (2006) AGL24, SHORT VEGETATIVE PHASE, and APETALA1 redundantly control AGAMOUS during early stages of flower development in *Arabidopsis*. Plant Cell **18:** 1373–1382

Grennan AK (2006) Genevestigator: facilitating Web-based gene-expression analysis. Plant Physiol **141:** 1164–1166

Hardtke CS, Berleth T (1998) The Arabidopsis gene MONOPTEROS encodes a transcription factor mediating embryo axis formation and vascular development. EMBO J **17:** 1405–1411

Jurata LW, Gill GN (1997) Functional analysis of the nuclear LIM domain interactor NLI. Mol Cell Biol **17:** 5688–5698

Jurata LW, Kenny DA, Gill GN (1996) Nuclear LIM interactor, a rhombotin and LIM homeodomain interacting protein, is expressed early in neuronal development. Proc Natl Acad Sci USA **93:** 11693–11698

Klucher KM, Chow H, Reiser L, Fischer RL (1996) The *AINTEGUMENTA* gene of *Arabidopsis* required for ovule and female gametophyte development is related to the floral homeotic gene *APETALA2*. Plant Cell **8:** 137–153

Liu Z, Franks RG, Klink VP (2000) Regulation of gynoecium marginal tissue formation by *LEUNIG* and *AINTEGUMENTA*. Plant Cell **12:** 1879–1892

Liu Z, Meyerowitz EM (1995) *LEUNIG* regulates *AGAMOUS* expression in *Arabidopsis* flowers. Development **121:** 975–991

Long JA, Moan EI, Medford JI, Barton MK (1996) A member of the *KNOTTED* class of homeodomain proteins encoded by the *STM* gene of *Arabidopsis*. Nature **379:** 66–69

Matthews JM, Visvader JE (2003) LIM-domain-binding protein 1: a multifunctional cofactor that interacts with diverse proteins. EMBO Rep **4:** 1132–1137

Morcillo P, Rosen C, Baylies MK, Dorsett D (1997) Chip, a widely expressed chromosomal protein required for segmentation and activity of a remote wing margin enhancer in *Drosophila*. Genes Dev **11:** 2729–2740

Navarro C, Efremova N, Golz JF, Rubiera R, Kuckenberg M, Castillo R, Tietz O, Saedler H, Schwarz-Sommer Z (2004) Molecular and genetic interactions between STYLOSA and GRAMINIFOLIA in the control of Antirrhinum vegetative and reproductive development. Development **131:** 3649–3659

Nishimura T, Wada T, Yamamoto KT, Okada K (2005) The *Arabidopsis* STV1 protein, responsible for translation reinitiation, is required for auxin-mediated gynoecium patterning. Plant Cell **17:** 2940–2953

Nole-Wilson S, Krizek BA (2006) AINTEGUMENTA contributes to organ polarity and regulates growth of lateral organs in combination with YABBY genes. Plant Physiol **141:** 977–987

Okada K, Ueda J, Komaki MK, Bell CJ, Shimura Y (1991) Requirement of the auxin polar transport system in early stages of *Arabidopsis* floral bud formation. Plant Cell **3:** 677–684

Pfluger J, Zambryski P (2004) The role of SEUSS in auxin response and floral organ patterning. Development **131:** 4697–4707

Przemeck GK, Mattsson J, Hardtke CS, Sung ZR, Berleth T (1996) Studies on the role of the Arabidopsis gene MONOPTEROS in vascular development and plant cell axialization. Planta **200:** 229–237

Saitou N, Nei M (1987) The neighbor-joining method: a new method for reconstructing phylogenetic trees. Mol Biol Evol **4:** 406–425

Schneitz K, Hulskamp M, Pruitt RE (1995) Wild-type ovule development in Arabidopsis thaliana: a light-microscope study of cleared whole-mount tissue. Plant J **7:** 731–749

Scofield S, Dewitte W, Murray JA (2007) The KNOX gene SHOOT MERISTEMLESS is required for the development of reproductive meristematic tissues in Arabidopsis. Plant J **50:** 767–781

Sessions A, Nemhauser JL, McColl A, Roe JL, Feldmann KA, Zambryski PC (1997) *ETTIN* patterns the *Arabidopsis* floral meristem and reproductive organs. Development **124:** 4481–4491

Sessions RA, Zambryski PC (1995) *Arabidopsis* gynoecium structure in the wild and in *ettin* mutants. Development **121:** 1519–1532

Shani E, Yanai O, Ori N (2006) The role of hormones in shoot apical meristem function. Curr Opin Plant Biol **9:** 484–489

Sitaraman J, Bui M, Liu Z (2008) LEUNIG_HOMOLOG and LEUNIG perform partially redundant functions during Arabidopsis embryo and floral development. Plant Physiol **147:** 672–681

Smyth DR, Bowman JL, Meyerowitz EM (1990) Early flower development in *Arabidopsis*. Plant Cell **2:** 755–767

Sridhar VV, Surendrarao A, Gonzalez D, Conlan RS, Liu Z (2004) Transcriptional repression of target genes by LEUNIG and SEUSS, two interacting regulatory proteins for Arabidopsis flower development. Proc Natl Acad Sci USA **101:** 11494–11499

Sridhar VV, Surendrarao A, Liu Z (2006) APETALA1 and SEPALLATA3 interact with SEUSS to mediate transcription repression during flower development. Development **133:** 3159–3166

Stahle MI, Kuehlich J, Staron L, von Arnim AG, Golz JF (2009) YABBYs and the transcriptional corepressors LEUNIG and LEUNIG_HOMOLOG maintain leaf polarity and meristem activity in Arabidopsis. Plant Cell **21:** 3105–3118

Stepanova AN, Robertson-Hoyt J, Yun J, Benavente LM, Xie DY, Dolezal K, Schlereth A, Jurgens G, Alonso JM (2008) TAA1-mediated auxin biosynthesis is essential for hormone crosstalk and plant development. Cell **133:** 177–191

Tamura K, Dudley J, Nei M, Kumar S (2007) MEGA4: Molecular Evolutionary Genetics Analysis (MEGA) software version 4.0. Mol Biol Evol **24:** 1596–1599

Tao Y, Ferrer JL, Ljung K, Pojer F, Hong F, Long JA, Li L, Moreno JE, Bowman ME, Ivans LJ, et al (2008) Rapid synthesis of auxin via a new tryptophan-dependent pathway is required for shade avoidance in plants. Cell **133:** 164–176

Thaler JP, Lee SK, Jurata LW, Gill GN, Pfaff SL (2002) LIM factor Lhx3 contributes to the specification of motor neuron and interneuron identity through cell-type-specific protein-protein interactions. Cell **110:** 237–249

Ulmasov T, Murfett J, Hagen G, Guilfoyle TJ (1997) Aux/IAA proteins repress expression of reporter genes containing natural and highly active synthetic auxin response elements. Plant Cell **9:** 1963–1971

van Meyel DJ, Thomas JB, Agulnick AD (2003) Ssdp proteins bind to LIM-interacting co-factors and regulate the activity of LIM-homeodomain protein complexes *in vivo*. Development **130:** 1915–1925

Zhao Y, Christensen SK, Fankhauser C, Cashman JR, Cohen JD, Weigel D, Chory J (2001) A role for flavin monooxygenase-like enzymes in auxin biosynthesis. Science **291:** 306–309

Zimmermann P, Hirsch-Hoffmann M, Hennig L, Gruissem W (2004) GENEVESTIGATOR: Arabidopsis microarray database and analysis toolbox. Plant Physiol **136:** 2621–2632

Zuckerkandl E, Pauling L (1965) Evolving Genes and Proteins. Academic Press, New York